Clim. Past Discuss., doi:10.5194/cp-2016-103, 2016
Manuscript under review for journal Clim. Past
Published: 24 October 2016

Estimation of pre-industrial nitrous oxide emissions from the land biosphere

Rongting Xu[1], Hanqin Tian[1], Chaoqun Lu[2,1], Shufen Pan[1], Jian Chen[3,1], Jia Yang[1], Bowen Zhang[1]

[1] International Center for Climate and Global Change Research and School of Forestry and Wildlife Sciences, Auburn University, Auburn, AL 36849, USA

[2] Department of Ecology, Evolution, & Organismal Biology, Iowa State University, Ames, IA 50011, USA

[3] College of Sciences and Mathematics, Auburn University, Auburn, AL 36849, USA

Correspondence to: Hanqin Tian (tianhan@auburn.edu)

Abstract. To accurately assess how increased global nitrous oxide (N_2O) emission has affected the climate system requires a robust estimation of the pre-industrial N_2O emissions since only the difference between current and pre-industrial emissions represents net drivers of anthropogenic climate change. However, large uncertainty exists in previous estimates of pre-industrial N_2O emissions from the land biosphere, while pre-industrial N_2O emissions at the finer scales such as regional, biome, or sector have not yet well quantified. In this study, we applied a process-based Dynamic Land Ecosystem Model (DLEM) to estimate the magnitude and spatial patterns of pre-industrial N_2O fluxes at the biome-, continental-, and global-level as driven by multiple environmental factors. Uncertainties associated with key parameters were also evaluated. Our study indicates that the mean of the pre-industrial N_2O emission was approximately 6.20 Tg N yr^{-1}, with an uncertainty range of 4.76 to 8.13 Tg N yr^{-1}. The estimated N_2O emission varied significantly at spatial- and biome-levels. South America, Africa, and Southern Asia accounted for 34.12%, 23.85%, 18.93%, respectively, together contributing of 76.90% of global total emission. The tropics were identified as the major source of N_2O released into the atmosphere, accounting for 64.66% of the total emission. Our multi-scale estimates with a reasonable uncertainty range provides

Clim. Past Discuss., doi:10.5194/cp-2016-103, 2016
Manuscript under review for journal Clim. Past
Published: 24 October 2016

a robust reference for assessing the climate forcing of anthropogenic N_2O emission from the land biosphere.

1 Introduction

Nitrous oxide (N_2O) acts as the third-most important greenhouse gas (GHG) after carbon dioxide (CO_2) and methane, contributing to the current radiative forcing (Myhre et al., 2013). Nitrous oxide is also the most long-lived reactant, resulting in the destruction of stratospheric ozone (Prather et al., 2015; Ravishankara et al., 2009). The atmospheric concentration of N_2O increased from 275 to 329 parts per billion (ppb) since the pre-industrial era until 2015 at a rate of approximately 0.26% per year, as a result of human activities (Davidson, 2009; Forster et al., 2007; NOAA2006A). The human-induced N_2O emissions together with methane emissions from the terrestrial biosphere have offset terrestrial CO_2 sink and contributed a net warming effect on the climate system (Tian et al., 2016). In the contemporary period, anthropogenic N_2O emissions are mainly caused by the expansion in agricultural land area and increase in fertilizer application, as well as industrial activities, biomass burning and indirect emissions from reactive nitrogen (N) (Galloway et al., 2004; Reay et al., 2012). Natural terrestrial ecosystems contribute more than half of N_2O released into the atmosphere when removing oceanic contribution (Denman et al., 2007). As some N_2O emissions were present during pre-industrial times, only the difference between current and pre-industrial emissions represents net drivers of anthropogenic climate change (Tian et al., 2016). Therefore, it is necessary to provide a robust reference of pre-industrial N_2O emission for assessing the climate forcing of anthropogenic N_2O emission from the land biosphere.

Clim. Past Discuss., doi:10.5194/cp-2016-103, 2016
Manuscript under review for journal Clim. Past
Published: 24 October 2016

Numerous studies have reported the sources and estimates of N_2O emission since the pre-industrial era (Davidson and Kanter, 2014; Galloway et al., 2004; Kroeze et al., 1999; Syakila and Kroeze, 2011). According to the Intergovernmental Panel on Climate Change Guidelines (IPCC, 1997), the global N_2O emission evaluated by Kroeze et al. (1999) is 11 (8–13) Tg N yr^{-1} (Natural soils: 5.6–6.6 Tg N yr^{-1}, Anthropogenic: 1.4 Tg N yr^{-1}), which is consistent with the estimation from global pre-agricultural N_2O emissions in soils (6–7 Tg N yr^{-1}) (Bouwman et al., 1993). While taking into account the new emission factor from the IPCC 2006 Guidelines (Denman et al., 2007), Syakila and Kroeze (2011) conducted an updated estimate based on the study of Kroeze et al. (1999) and reported that the global pre-industrial N_2O emission is 11.6 Tg N yr^{-1} (Anthropogenic: 1.1 Tg N yr^{-1}, Natural soils: 7 Tg N yr^{-1}). Based on the IPCC AR5, Davidson and Kanter (2014) indicated that the central estimates of both top-down and bottom-up approaches for pre-industrial natural emissions were in agreement at 11 (10–12) Tg N yr^{-1}, including natural emission from soils at 6.6 (3.3–9.0) Tg N yr^{-1} (Syakila and Kroeze, 2011). Although these previous estimates intent to provide a baseline of pre-industrial N_2O emission at global-level, information on pre-industrial N_2O emissions on fine resolutions such as biome-, sector- or country-, and regional-levels remains unknown but needed for climate change mitigation.

Large uncertainties in the estimates of pre-industrial N_2O emission could derive from different approaches (i.e. top-down and bottom-up), as mentioned above. Nitrous oxide, as an important component of the N cycle, is produced by biological processes such as denitrification and nitrification in terrestrial and aquatic systems (Schmidt et al., 2004; Smith and Arah, 1990; Wrage et al., 2001). In order to accurately estimate pre-industrial N_2O emissions using the process-based Dynamic Land Ecosystem Model (DLEM, Tian et al., 2010), uncertainties associated with key parameters, such as maximum

Clim. Past Discuss., doi:10.5194/cp-2016-103, 2016
Manuscript under review for journal Clim. Past
Published: 24 October 2016

nitrification and denitrification rates, biological N fixation (BNF) rates, and the adsorption coefficient for soil ammonium (NH_4^+) and nitrate (NO_3^-), were required to be considered in model simulation. Upper and lower limits of these parameters were used to derive a range of pre-industrial N_2O emissions from terrestrial ecosystems.

In this study, the DLEM was used to simulate global N_2O emission in the pre-industrial era at a resolution of 0.5° × 0.5° latitude/longitude. Since there is no observational data of N_2O emission in the pre-industrial period, a simple atmospheric box model (one-box) was applied to validate the estimated N_2O emissions from DLEM simulations. We calculated trends of N_2O concentrations during 1860–2006 through accounting for all possible N_2O sources from land biosphere and marine ecosystems based on the previous publications. Then, the observational atmospheric N_2O concentrations from monitoring stations during 1977–2006 were used to compare with the calculated concentrations from the one-box model. Finally, our estimates at global- and biome-scales were compared with previous estimates.

2 Methodology

2.1 Model description

The DLEM is a highly integrated process-based ecosystem model, which combines biophysical characteristics, plant physiological processes, biogeochemical cycles, vegetation dynamics and land use to make daily, spatially-explicit estimates of carbon, nitrogen and water fluxes and pool sizes in terrestrial ecosystems from site- and regional- to global-scales (Lu and Tian, 2013; Tian et al., 2012). The DLEM is characterized of cohort structure, multiple soil layer processes, coupled carbon, water and nitrogen cycles, multiple GHG emissions simulation, enhanced land surface processes, and dynamic linkages

Clim. Past Discuss., doi:10.5194/cp-2016-103, 2016
Manuscript under review for journal Clim. Past
Published: 24 October 2016

between terrestrial and riverine ecosystems (Liu et al., 2013; Tian et al., 2015; Tian et al., 2010). The previous results of GHG emissions from DLEM simulations have been validated against field observations and measurements at various sites (Lu and Tian, 2013; Ren et al., 2011; Tian et al., 2010; Tian et al., 2011; Zhang et al., 2016). The estimates of water, carbon, and nutrients fluxes and storages were also compared with the estimates from different approaches at regional-, continental-, and global-scales (Pan et al., 2014; Tian et al., 2015; Yang et al., 2015). Different soil organic pools and calculations of decomposition rates were described in Tian et al. (2015). The decomposition and nitrogen mineralization processes in the DLEM were described in other publications (Lu and Tian, 2013; Yang et al., 2015).

The N_2O module

Previous work provided a detailed description of trace gas modules in the DLEM (Tian et al., 2010). However, both denitrification and nitrification processes have been modified based on the first-order kinetics (Chatskikh et al., 2005; Heinen, 2006).

In the DLEM, the N_2O production and fluxes are determined by soil inorganic N content (NH_4^+ and NO_3^-) and environmental factors, such as soil texture, temperature, and moisture:

$$F_{N2O} = (R_{nit} + R_{den})F(T_{soil})(1 - F(Q_{wfp})) \quad (1)$$

where F_{N2O} is the N_2O flux from soils to the atmosphere (g N m^2 d^{-1}), R_{nit} is the daily nitrification rate (g N m^2 d^{-1}), R_{den} is the daily denitrification rate (g N m^2 d^{-1}), $F(T_{soil})$ is the function of daily soil temperature on nitrification process (unitless), and $F(Q_{wfp})$ is the function of water-filled porosity (unitless).

Clim. Past Discuss., doi:10.5194/cp-2016-103, 2016
Manuscript under review for journal Clim. Past
Published: 24 October 2016

Nitrification, a process converting NH_4^+ into NO_3^-, is simulated as a function of soil temperature, moisture, and soil NH_4^+ concentration:

$$R_{\mathrm{nit}} = k_{\mathrm{nit}} F(T_{\mathrm{soil}}) F(\psi) C_{\mathrm{NH_4}} \quad (2)$$

where k_{nit} is the daily maximum fraction of NH_4^+ that is converted into NO_3^- or gases (d^{-1}), $F(\psi)$ is the soil moisture effect (unitless), and $C_{\mathrm{NH_4}}$ is the soil NH_4^+ content (g N m^{-2}). Unlike Chatskikh *et al* 2005, who set k_{nit} to 0.10 d^{-1}, it varies with different plant function types (PFTs) in the DLEM with a range of 0.04 to 0.15 d^{-1}. The detailed calculations of $F(T_{\mathrm{soil}})$ and $F(\psi)$ were described in Pan et al. (2015) and Yang et al. (2015).

Denitrification is the process that converts NO_3^- into three types of gases, namely, nitric oxide, N_2O, dinitrogen. The denitrification rate is simulated as a function of soil temperature, water-filled porosity, and NO_3^- concentration $C_{\mathrm{NO_3}}$ (g N g^{-1} soil):

$$R_{\mathrm{den}} = \alpha F(T_{\mathrm{soil}}) F(Q_{\mathrm{wfp}}) F_{\mathrm{N}}(C_{\mathrm{NO_3}}) \quad (3)$$

where $F_{\mathrm{N}}(C_{\mathrm{NO_3}})$ is the dependency of the denitrification rate on NO_3^- concentration (unitless), and α is the maximum denitrification rate (g N m^{-2} d^{-1}). The detailed calculations of $F(Q_{\mathrm{wfp}})$, $F_{\mathrm{N}}(C_{\mathrm{NO_3}})$ and α were described in Yang et al. (2015).

In each grid cell, there are four natural vegetation types and one crop type. The sum of N_2O emission in each grid/d^{-1} is calculated by the following formula:

$$E = \sum_{i=1}^{62481} \sum_{j=1}^{5} \left(N_{ij} \times f_{ij}\right) \times A_i \times 10^6/10^{12}, \; i = 1, \cdots, 62481, j = 1, \cdots, 5 \quad (4)$$

Clim. Past Discuss., doi:10.5194/cp-2016-103, 2016
Manuscript under review for journal Clim. Past
Published: 24 October 2016

where E is the daily sum of N_2O emission from all plant functional types (PFTs) in total grids (Tg N/yr^{-1} d^{-1}); N_{ij} (g N/m^2) is the N_2O emission in the grid cell i for PFT j; f_{ij} is the fraction of cell used for PFT j in grid cell i; and A_i (km^2) is the area of the ith grid cell. 10^6 is to convert km^2 to m^2 and 10^{12} is to convert g to Tg.

2.2 Input datasets

Input data to drive DLEM simulation include static and transient data (Tian et al., 2010). Several additional data sets were generated to better represent terrestrial environment in the pre-industrial period as described below. The natural vegetation map was developed based on LUH (Hurtt et al., 2011) and SYNMAP (Jung et al., 2006), which rendered the fractions of 47 vegetation types in each 0.5° grid. These 47 vegetation types were converted to 15 PFTs used in the DLEM through a cross-walk table (Figure 1). Cropland distribution in 1860 were developed by aggregating the 5-arc minute resolution HYDE v3.1 global cropland distribution data (Figure 2). Half degree daily climate data (including average, maximum, minimum air temperature, precipitation, relative humidity, and shortwave radiation) were derived from CRU-NCEP climate forcing data (Wei et al., 2014). As global climate dataset was not available prior to the year 1900, long-term average climate datasets from 1901 to 1930 were used to represent the initial climate state in 1860. The nitrogen deposition dataset was developed based on the atmospheric chemistry transport model (Dentener, 2006) constrained by the EDGAR-HYDE nitrogen emission data (Aardenne et al., 2001). The nitrogen deposition dataset provided inter-annual variations of NH_x-N and NO_y-N deposition rates. The manure production dataset (1961–2013) was derived from Food and Agriculture organization of the United Nations statistic website ((FAO), http://faostat.fao.org) and defaulted for N

Clim. Past Discuss., doi:10.5194/cp-2016-103, 2016
Manuscript under review for journal Clim. Past
Published: 24 October 2016

excretion rate referred to IPCC Guidelines (Zhang et al., in preparation). Estimates of manure production from 1860 to 1960 were retrieved from the global estimates in (Holland et al., 2005).

2.3 Model simulation

The implementation of the DLEM simulation includes three steps: (1) equilibrium run, (2) spinning-up run, and (3) transient run. In this study, we first used land use and land cover (LULC) map in 1860, long-term mean climate during 1901–1930, N input datasets in 1860 (the concentration levels of N deposition and manure application rate), and atmospheric CO_2 in 1860 to run the model to an equilibrium state. In each grid, the equilibrium state was assumed to be reached when the inner-annual variations of carbon, nitrogen, and water storage are less than 0.1 g C/m^2, 0.1 g N/m^2 and 0.1 mm, respectively, during two consecutive 50 years. After the model reached equilibrium state, the model was spun up by the detrended climate data from 1901 to 1930 to eliminate system fluctuation caused by the model mode shift from the equilibrium to transient run (i.e., 3 spins with 10-year climate data each time). Finally, the model was run in the transient mode with daily climate data, annual CO_2 concentration, manure application, and N deposition inputs in 1860 to simulate pre-industrial N_2O emissions. Additional description of model initialization and simulation procedure can be found in previous publications (Tian et al., 2010).

2.4 Model validation

2.4.1 Comparison with field measurements

Observations of annual N_2O emission accumulations (g N m^{-2} yr^{-1}) were selected to compare with the simulated emissions in different sites. As there were no field measurements in the pre-industrial era, observations during 1970–2009 were collected to test the model performance in the contemporary period.

Clim. Past Discuss., doi:10.5194/cp-2016-103, 2016
Manuscript under review for journal Clim. Past
Published: 24 October 2016

All environmental factors (climate, CO_2 concentration, soil property, N deposition, LULC) in the exact year were used as input datasets for N_2O simulations. The selected sites include temperate forest, tropical forest, boreal forest, savanna, and grassland globally. As shown in Figure 3, the simulated N_2O emissions have a good correlation with field observations (R^2 = 0.79). It indicates that the DLEM has capacity to simulate N_2O emissions in the pre-industrial era driven by environmental factors back then. The detailed information at each site can be found in Table 1S.

2.4.2 One-box model validation

A one-box model was used to estimate the accuracy of N_2O fluxes from DLEM simulations (Kroeze et al., 1999). The model equation is as follows:

$$dC/dt = S/F - C/T \quad (5)$$

where C is concentration (ppb), S is emissions (Tg N), T is atmospheric lifetime (years), t is time (years), and F conversion factor (Tg N ppb^{-1}).

Atmospheric N_2O concentration in 1860 derived from the records of Antarctic ice core was about 275 (263–280) ppb (Machida et al., 1995; Prather et al., 2012; Rahn and Wahlen, 2000; Spahni et al., 2005). The atmospheric N_2O concentration in 2006 was measured as about 320 ppb, which is approximately 18–20% higher than its pre-industrial value (Ciais et al., 2014). The atmospheric lifetime of N_2O was 114 years, with a range of 106 to 141 years (Ciais et al., 2014; Prather et al., 2012; Prather and Hsu, 2010; Volk et al., 1997).

The initial N_2O concentration in the one-box atmospheric model was set as 275 ppb. F conversion factor is 4.8 Tg N ppb^{-1} adopted from Kroeze et al. (1999). The atmospheric lifetime of N_2O was set as

Clim. Past Discuss., doi:10.5194/cp-2016-103, 2016
Manuscript under review for journal Clim. Past
Published: 24 October 2016

114 years. The mean with 95% confidence intervals, the maximum, and minimum values of estimates from DLEM simulations were applied as initial emissions to calculate the atmospheric N_2O concentration in 2006 as shown in Table 1 (Scenarios 1–4 and baseline), as well as concentration changes from 1860 to 2006, as shown in Figure 7. According to the NOAA2006A, the monthly records of atmospheric N_2O concentrations from different monitoring stations globally were from 1977 to 2015. Thus, the observed trends from three stations: Pt. Barrow, Alaska, USA (71.3N, 156.6W), Mauna Loa, Hawaii, USA (19.5N, 155.6W), and South Pole (90S), were used to compare the calculated trends from all the above scenarios during 1977 to 2006 (Figure 7). As uncertainties exist in the N_2O concentration from ice core records and the determination of its lifetime, the minimum and maximum estimates of them were used to calculate the ranges of N_2O concentrations in 2006, as shown in Table 1 (Scenarios 5–6).

2.5 Estimate of uncertainty

In this study, uncertainties in the simulated N_2O emission were evaluated through a global sensitivity and uncertainty analysis (Tian et al., 2011). Based on sensitivity analyses of key parameters that affect terrestrial N_2O fluxes, the most sensitive parameters were identified to conduct uncertainty simulations in the DLEM, such as potential denitrification and nitrification rates, BNF rates, and the adsorption coefficient for soil NH_4^+ and NO_3^- (Gerber et al., 2010; Tian et al., 2015;Yang et al., 2015). The ranges of five parameters were obtained from previous studies. Chatskikh et al. (2005) set k_{nit} as 0.10 d^{-1}; however, it was set in a range of 0.04 to 0.15 d^{-1}, and varied with different PFTs in the DLEM simulations. The uncertainty ranges of potential nitrification rates were based on previous studies (Hansen, 2002; Heinen, 2006); the global pre-industrial N fixation was estimated as 58 Tg N yr^{-1}, ranging from 50–100 Tg N yr^{-1} (Vitousek et al., 2013). The spatial distribution of BNF referred to estimates done by Cleveland et al.

Clim. Past Discuss., doi:10.5194/cp-2016-103, 2016
Manuscript under review for journal Clim. Past
Published: 24 October 2016

(1999). Potential denitrification rate was set in an uncertainty range of 0.025–0.74 d^{-1}, and varied with different PFTs in the DLEM. The uncertainty ranges of the adsorption coefficient were referred to the sensitivity analysis conducted in Yang et al. (2015). Parameters used in the DLEM simulations for uncertainty analysis were assumed to follow a normal distribution. The Improved Latin Hypercube Sampling (LHS) approach was used to randomly select an ensemble of 100 sets of parameters (R version 3.2.1) (Tian et al., 2015; Tian et al., 2011).

In the DLEM, after the model reached equilibrium state, a spinning-up run was implemented using de-trended climate data from 1901 to 1930 for each set of parameter values. Then, each set of the model was run in transient mode in 1860 to produce the result of the pre-industrial N_2O emissions. All results from 100 groups of simulations are shown in the Table 2S. The Shapiro–Wilk test was used on 100 sets of results to check the normality of DLEM simulations. It turned out that the distribution is not normal (P value < 0.05, R version 3.2.1), as shown in Figure 1S. Thus, the uncertainty range was represented as the minimum and maximum value of 100 sets of DLEM simulations. In order to speculate the distribution of the global mean N_2O emission, we conduct the replicated Bootstrap resampling method (Efron and Tibshirani, 1994) using 100 sets of DLEM simulation results. The 95% confidence intervals were constructed with 10,000 replicates for defining the uncertainty bounds of the estimates of the global mean N_2O emission (Figure 2S).

3 Results & discussion

3.1 Magnitude and spatial distribution of N_2O emission

Clim. Past Discuss., doi:10.5194/cp-2016-103, 2016
Manuscript under review for journal Clim. Past
Published: 24 October 2016

We define the parameter-induced uncertainty of our global estimates as a range between the minimum (4.76 Tg N yr^{-1}) and the maximum (8.13 Tg N yr^{-1}) of 100 sets of DLEM simulations. The global mean N_2O emission was 6.20 Tg N yr^{-1}, with 95% confidence intervals of 6.03 to 6.36 Tg N yr^{-1}. The terrestrial ecosystem in the pre-industrial period acted as a source of N_2O, and its spatial pattern mostly depends on the biome distribution across the global land surface. The spatial distribution of annual N_2O emission in a 0.5° × 0.5° grid (Figure 4) shows that the strong sources were found near the equator, such as Southeast Asia, Central Africa, and Central America, where N_2O emission reached as high as 0.45 g N m^{-2} yr^{-1}. The weak N_2O sources were observed in the northern areas of North America and Asia, where the estimated N_2O emission was less than 0.001 g N m^{-2} yr^{-1}. The microbial activity in soils determined the rate of nitrification and denitrification processes, which accounts for approximately 70% of global N_2O emissions (Smith and Arah, 1990; Syakila and Kroeze, 2011). The tropical regions near the equator could provide microbes optimum temperatures and soil moistures to decompose soil organic matter and release more NO_x and CO_2 into the atmosphere (Butterbach-Bahl et al., 2013). Referring to the observational data from field experiments and model simulations in the tropics, it has been supported that the tropics are the main sources within the total N_2O emissions from natural vegetation (Bouwman et al., 1995; Werner et al., 2007; Zhuang et al., 2012).

In this study, Asia is divided into two parts: Southern Asia and Northern Asia, where the PFTs and climate conditions are significantly contrasting. As shown in Figure 1, tropical forest and cropland were dominant PFTs in Southern Asia. In contrast, temperate and boreal forests were main PFTs in Northern Asia. The estimates of N_2O emissions from seven land regions are shown in Figure 5. At continental scales, the N_2O emission was 2.09 (1.63–2.73) Tg N yr^{-1} in South America, 1.46 (1.13–1.91) Tg N yr^{-1}

Clim. Past Discuss., doi:10.5194/cp-2016-103, 2016
Manuscript under review for journal Clim. Past
Published: 24 October 2016

in Africa, and 1.16 (0.90–1.52) Tg N yr^{-1} in Southern Asia. South America, Africa, and Southern Asia accounted for 33.77%, 23.60%, 18.73%, respectively, together which was 76.10% of global total emission. Europe and Northern Asia contributed to 0.45 (0.32–0.66) Tg N yr^{-1}, which was less than 10% of the total emission.

Nitrous oxide emissions varied remarkably among different ecosystems. Forest, grassland, shrub, tundra and cropland contributed 76.90%, 3.11%, 13.14%, 0.18% and 6.67%, respectively, to the total emission globally (Figure 6). In different biomes, the tropics accounted for more than half of the total N_2O emission, which is comparable to the conclusion made by Bouwman et al. (1993). In the pre-industrial era, the major inputs of reactive N to terrestrial ecosystems were from BNF, which relies on the activity of a phylogenetically diverse list of bacteria, archaea and symbioses (Cleveland et al., 1999; Vitousek et al., 2013). Tropical savannas have been considered as 'hot spots' of BNF by legume nodules that provide the major input of available N (Bate and Gunton, 1982). The substantial inputs of N into tropical forests could contribute to higher amount of the gaseous N losses as N_2O or nitrogen gas (Cleveland et al., 2010; Hall and Matson, 1999). In contrast, as the largest terrestrial biome, boreal forests lack of available N because the rate of BNF is constricted by cold temperatures and low precipitation during growing season (Alexander and Billington, 1986). Morse et al. (2015) conducted field experiments in Northeastern North American forests. They found that denitrification does vary coherently with patterns of N availability in forests, and no significant correlations between atmospheric N deposition, potential net N mineralization and nitrification rates. Thus, it is reasonable that boreal forests contributed to the least amount of N_2O emission among different forests.

Clim. Past Discuss., doi:10.5194/cp-2016-103, 2016
Manuscript under review for journal Clim. Past
Published: 24 October 2016

As shown in Figure 2, cropland areas varied spatially. The regions with high cropland area were the entire Europe, India, eastern China, and central-eastern United States. The global N_2O emission from croplands was estimated as 0.41 (0.32–0.55) Tg N yr^{-1}, which is about ten times less than the estimate reported in the IPCC AR5 (Ciais et al., 2014). As no synthetic N fertilizer was applied to the cropland in 1860, leguminous crops were the major source of N_2O emission from croplands, most of which were planted in central-eastern United States (Figure 4). Rochette et al. (2004) conducted the experiments on the N_2O emission from soybean without application of N fertilizer. Their work was in agreement with the suggestion that legumes may increase N_2O emissions compared with non-BNF crops (Duxbury et al., 1982) The background emission from ground-based experiments was as high as 0.31–0.42 kg N ha^{-1} in Canada (Duxbury et al., 1982; Rochette et al., 2004).

We estimated pre-industrial N_2O emissions from seventeen countries that are "hotspots" of N_2O sources in the contemporary period (Table 2). The order of countries was referred to Gerber et al. (2016) that indicated the top seventeen countries in terms of total N application in 2000. Pre-industrial N_2O emissions from natural soils and croplands varied significantly at country-scales. The United States, China, and India were top countries accounted for emissions from pre-industrial croplands. Countries close to or located in the tropics, such as Mexico, Indonesia, and Brazil, accounted for negligible emissions from croplands, but substantial amount from natural vegetation in the pre-industrial era. Previous studies indicated that agriculture produces the majority of anthropogenic N_2O emissions (Ciais et al., 2014; Davidson and Kanter, 2014). Our estimate at country-scales could be used as a reference to quantify the net increase of N_2O emissions from agriculture activities in countries of "hotspots".

Clim. Past Discuss., doi:10.5194/cp-2016-103, 2016
Manuscript under review for journal Clim. Past
Published: 24 October 2016

There is a debate that the natural wetlands and peatlands act as sinks or sources of N_2O. Previous studies showed that N_2O emissions from natural peatlands are usually negligible; however, the drained peatlands with lower water tables might act as sources of N_2O (Augustin et al., 1998; Martikainen et al., 1993). High water tables in wetlands might block the activity of nitrifiers and limit the denitrification (Bouwman et al., 1993). The fluxes of N_2O were negligible in the pelagic regions of boreal ponds and lakes due to the limitation of nitrification and/or nitrate inputs (Huttunen et al., 2003). Couwenberg et al. (2011) mentioned that N_2O emissions always decreased after rewetting when conducting field experiments, which had been excluded from their future analysis of GHG emissions in peatlands. Hadi et al. (2005) pointed out that tropical peatlands ranged from sources to sinks of N_2O, highly affected by land-use and hydrological zone. In 1860, we were incapable to examine N_2O fluxes from wetlands and peatlands as human-induced land-use in those ecosystems was unknown. Thus, we excluded the N_2O emissions from wetlands and peatlands in this study.

3.2 Validation of DLEM results using the one-box model

The sources of N_2O include direct and indirect emissions. All anthropogenic emissions of N_2O in 1860, although in a low rate, were discussed in Davidson (2009), which included all direct emission from biomass burning, fossil fuel combustion, etc. The net anthropogenic source in their work was estimated as 0.42 Tg N yr^{-1} in the pre-industrial period. However, the indirect emissions from the riverine induced by the leaching and runoff of manure applications in agro-ecosystems, legume crop N fixation, and human sewage discharging have not been addressed in Davidson (2009). According to the IPCC 1997, indirect N_2O emission was estimated as the total N leaching or runoff multiplied the emission factors. Through

Clim. Past Discuss., doi:10.5194/cp-2016-103, 2016
Manuscript under review for journal Clim. Past
Published: 24 October 2016

combining the estimates from Davidson (2009) and emission factors from the IPCC 1997, the pre-industrial indirect emission (Tg N yr^{-1}) was calculated as follows:

$$\text{Indirect } N_2O \text{ emission} = 0.3 \times (15 + 26.3 + 4.7) \times (0.015 + 0.0075 + 0.0025) = 0.35$$

where 0.3 is the percentage of N through leaching or runoff (Sawamoto et al., 2005); 15, 26.3, and 4.7 Tg N are the amount of crop fixed N, manure N, and human sewage N in the preindustrial era, respectively (Davidson, 2009); 0.015, 0.0075, and 0.0025 are emission factors for degassing after discharge to surface waters, in rivers, and in estuaries, respectively (IPCC 1997). Thus, the total emission from anthropogenic activities in 1860 was estimated as 0.77 Tg N yr^{-1}, which was shown in Table 1. Syakila and Kroeze (2011) assumed that N_2O emission from oceans was 3.5 Tg N yr^{-1}, which had increased 1 Tg N yr^{-1} since 1950 and was static at 4.5 Tg N yr^{-1} from 2000–2006. In this study, N_2O emission atmospheric sources were assumed to be steady over time (Ciais et al., 2014). The net anthropogenic N_2O emission in 2006 was estimated as 7.2 Tg N yr^{-1} (Syakila and Kroeze, 2011). Annual increase of net human-induced N_2O emission was listed in Table 3S. All above possible sources of N_2O emission in 1860 were used to calculate the total emission, as listed in Table 1. The detailed calculation of the total emission in 1860 and 2006 can be found in the supplementary material.

As indicated by the calculated N_2O concentration in 2006 for different scenarios (Table 1), the estimated mean global N_2O emission of 320.16 ppb was close to the observed concentrations in three monitoring stations (MLO: 320.87; BRW: 320.73; SPO: 319.52 ppb) (NOAA2006A). However, the increasing trends from monitoring stations and the one-box model calculations differed from each other. The calculated increase rates of N_2O concentrations from model calculation were higher than the observed

Clim. Past Discuss., doi:10.5194/cp-2016-103, 2016
Manuscript under review for journal Clim. Past
Published: 24 October 2016

increase rates during 1977–1995. After the year 1995, the yearly increase rates from model calculations and observations were similar, as shown in Figure 7. The calculated concentration in 2006 from the upper and lower bound of the global mean is 318.02 and 322.30 ppb. The maximum concentration from the range of global mean emission was slightly lower than the calculation in Syakila and Kroeze (2011). It is because the initial and total emission (11.6; 19.8 Tg N yr^{-1}) from their study were higher than the estimates (11.23; 19.43 Tg N yr^{-1}) in this study. The calculated N_2O concentrations in 2006 from scenario 3 is 304.61 ppb, which is much lower than the current concentration. Similarly, the result from scenario 4 is much higher than the observed N_2O concentrations. Thus, we can conclude that the best estimate of N_2O emission from pre-industrial global soils was around 6.20 (6.03–6.36) Tg N yr^{-1}. The extremely lower or higher estimates could not reflect the real N_2O emission from terrestrial ecosystems under little human perturbation.

The uncertainty ranges in atmospheric lifetime and initial concentration could influence the calculation of atmospheric N_2O concentration in 2006, as well as the trend of concentration changes since 1860. As shown in Table 1, lower lifetime resulted in the lower value of atmospheric N_2O concentration, and vice versa. Similarly, lower initial atmospheric concentration resulted in lower estimate of atmospheric N_2O concentration in 2006, and vice versa, while the effect is less significant than lifetime. Overall, we provide a reasonable estimation of N_2O emission from the pre-industrial global soils in the context that the N_2O concentration was 275 ppb and lifetime was set as 114 years.

3.3 Comparison with other studies

Clim. Past Discuss., doi:10.5194/cp-2016-103, 2016
Manuscript under review for journal Clim. Past
Published: 24 October 2016

The global pre-agricultural N_2O emission was estimated as 6.8 Tg N yr^{-1} based on the regression relationship between measured N_2O fluxes and modeled N_2O production indices (Bouwman et al., 1993). This estimate was adopted to retrieve the trends of atmospheric N_2O concentration in Syakila and Kroeze (2011). In our study, the pre-industrial N_2O emission from natural vegetation was estimated as 5.78 (4.4–7.72) Tg N yr^{-1}, which is about 1 Tg N yr^{-1} lower than the estimate from Bouwman et al. (1993). Estimate from the tropics (± 30° of the equator) was about 4.57 Tg N yr^{-1}, which is 0.83 Tg N yr^{-1} lower than the estimate from Bouwman et al. (1993). For the rest of natural vegetation, our estimate was 1.21 Tg N yr^{-1}, which is close to 1.4 Tg N yr^{-1} estimated in Bouwman et al. (1993).

Although Bouwman et al. (1993) has studied the potential N_2O emission from natural soils, our study provided a first estimate of spatially distributed N_2O emission in 1860 using the biogeochemical process-based model. Bouwman et al. (1993) provided 1° × 1° monthly N_2O emission using the monthly controlling factors without considering the impact of N deposition. In their study, the soil fertility and carbon content were constant for every month, which could not reflect the monthly dynamic changes of carbon and N pools in natural soils. Moreover, although their study has represented a spatial distribution of potential N_2O emission from natural soils, they had not provided the estimate at biome-, continent-, and country-scales. Thus, their result was hardly to be used as a regional reference for the net human-induced N_2O emissions from some “hotspots”, such as Southern Asia. In contrast, in our study, using daily climate and N deposition dataset could better reflect the real variation of N_2O emission through the growing season in natural ecosystems. The comparison with field observations during 1997–2001 indicated that the DLEM can catch the daily peak N_2O emissions in Hubbard Brook Forest (Tian et al., 2010) and Inner-Mongolia (Tian et al., 2011).

Clim. Past Discuss., doi:10.5194/cp-2016-103, 2016
Manuscript under review for journal Clim. Past
Published: 24 October 2016

As far as the N_2O emission from croplands, our estimate is comparable to the estimate of 0.3 (0.29–0.35) Tg N yr^{-1} extracted from Syakila and Kroeze (2011) by digitizing graphs using the Getdata Graph Digitizer (version 2.6.2, Russian Federation). In their study, the estimation was based on the relationship between the crop production and human population during 1500–1970. In contrast, the result in our study was estimated based on the cropland area of specific crop type, mainly soybean, rice, corn, and wheat in 1860.

Thus, the DLEM is capable to provide the estimate of N_2O emission at regional- and biome-scales with a higher spatial resolution, which could be a useful reference for studying how the LULC change, such as tropical forest deforestation (Davidson, 2009), N fertilizer and manure application, and increasingly atmospheric N deposition affect N_2O emissions in different terrestrial ecosystems or sectors in the contemporary period.

3.4 Future research needs

Large uncertainty still exists in the DLEM simulation associated with the quality of input datasets and parameters applied in simulations. Although input datasets could play a significant role in the variety of the model output, it is difficult to obtain accurate datasets back to the year 1860. Average climate data from 1901 to 1930 was used to run model simulation, which could raise the uncertainty in estimating N_2O emission in 1860. The datasets of LULC, N deposition, and manure application in 1860 could introduce uncertainties to this estimate. The estimates of human-induced N_2O emission could introduce the uncertainty into the calculation of the N_2O concentrations in 2006. Nitrous oxide emission from inland water system was calculated according to the empirical emission factor in the IPCC 1997. However, other

studies have indicated that the IPCC 1997 overestimated the indirect N_2O emission (Hu et al., 2016; Sawamoto et al., 2005). Thus, the estimate of indirect emission remains a large uncertainty. The N_2O fluxes from wetlands and peats needed to be included in the future study.

4 Conclusions

Using the process-based land ecosystem model DLEM, this study provides a spatially-explicit estimate of pre-industrial N_2O emissions for major PFTs across global land surface. The one-box model was used to calculate the atmospheric N_2O concentration in 2006 to validate the results from DLEM simulations. Improved LHS and Bootstrapping were performed to analyze uncertainty ranges of the estimates. We estimated that pre-industrial N_2O emission is 6.20 Tg N yr^{-1}. Calculated N_2O concentration in 2006 using the global mean N_2O emission was 320.16 ppb, which was similar to the observed values from three monitoring stations. The modeled results showed a large spatial variability due to variations in climate conditions and PFTs. Tropical ecosystems were the dominant contributors of global N_2O emissions. In contrast, boreal regions contributed less than 5% to the total emission. China, India and United States are top countries accounted for emissions from croplands in 1860. While uncertainties still exist in the N_2O emission estimation in the pre-industrial era, this study offered a relatively reasonable estimate of the pre-industrial N_2O emission from land soils. Meanwhile, this study provided a spatial estimate for N_2O emission from the global hotspots, which could be used as a reference to estimate net human-induced emissions in the contemporary period.

Clim. Past Discuss., doi:10.5194/cp-2016-103, 2016
Manuscript under review for journal Clim. Past
Published: 24 October 2016

Author Contributions

Xu R. performed DLEM simulations, analyses, calculations, and drafted the manuscript. Tian H. and Pan S. initiated this research and provided the comments for the whole work. Lu C. provided the idea of one-box model validation and contributed to the model calibration and data analysis. Chen J. contributed to the data processing and statistical analysis. Yang J. took charge of input datasets preparation (environmental factors), data description, and model verification. Zhang B. provided manure N input data and the comments on the manuscript.

Acknowledgements

This work was supported by National Science Foundation (NSF) Grants (1243232, 121036). We wish to thank the previous members in the International Center for Climate and Global Change Research who made great contributions to the improvements of the DLEM in the past decade.

References

Aardenne, J. V., Dentener, F., Olivier, J., Goldewijk, C., and Lelieveld, J.: A 1× 1 resolution data set of historical anthropogenic trace gas emissions for the period 1890–1990, Global Biogeochemical Cycles, 15, 909-928, 2001.

Alexander, V., and Billington, M.: Nitrogen fixation in the Alaskan taiga, in: Forest ecosystems in the Alaskan taiga, Springer, 112-120, 1986.

Augustin, J., Merbach, W., Steffens, L., and Snelinski, B.: Nitrous oxide fluxes of disturbed minerotrophic peatlands, Agribiological Research, 51, 47-57, 1998.

Bate, G., and Gunton, C.: Nitrogen in the Burkea savanna, in: Ecology of tropical savannas, Springer, 498-513, 1982.

Bouwman, A., Fung, I., Matthews, E., and John, J.: Global analysis of the potential for N_2O production in natural soils, Global Biogeochemical Cycles, 7, 557-597, 1993.

Bouwman, A., Van der Hoek, K., and Olivier, J.: Uncertainties in the global source distribution of nitrous oxide, Journal of Geophysical Research: Atmospheres, 100, 2785-2800, 1995.

Butterbach-Bahl, K., Baggs, E. M., Dannenmann, M., Kiese, R., and Zechmeister-Boltenstern, S.: Nitrous oxide emissions from soils: how well do we understand the processes and their controls?, Phil. Trans. R. Soc. B, 368, 20130122, 2013.

Chatskikh, D., Olesen, J. E., Berntsen, J., Regina, K., and Yamulki, S.: Simulation of effects of soils, climate and management on N_2O emission from grasslands, Biogeochemistry, 76, 395-419, 2005.

Ciais, P., Sabine, C., Bala, G., Bopp, L., Brovkin, V., Canadell, J., Chhabra, A., DeFries, R., Galloway, J., Heimann, M. and Jones, C.: Carbon and other biogeochemical cycles. In Climate Change 2013: The Physical Science Basis. Contribution of Working Group I to the Fifth Assessment Report of the Intergovernmental Panel on Climate Change. Cambridge University Press, 465-570, 2014.

Cleveland, C. C., Townsend, A. R., Schimel, D. S., Fisher, H., Howarth, R. W., Hedin, L. O., Perakis, S. S., Latty, E. F., Von Fischer, J. C., and Elseroad, A.: Global patterns of terrestrial biological nitrogen (N_2) fixation in natural ecosystems, Global Biogeochemical Cycles, 13, 623-645, 1999.

Cleveland, C. C., Houlton, B. Z., Neill, C., Reed, S. C., Townsend, A. R., and Wang, Y.: Using indirect methods to constrain symbiotic nitrogen fixation rates: a case study from an Amazonian rain forest, Biogeochemistry, 99, 1-13, 2010.

Couwenberg, J., Thiele, A., Tanneberger, F., Augustin, J., Bärisch, S., Dubovik, D., Liashchynskaya, N., Michaelis, D., Minke, M., and Skuratovich, A.: Assessing greenhouse gas emissions from peatlands using vegetation as a proxy, Hydrobiologia, 674, 67-89, 2011.

Davidson, E. A.: The contribution of manure and fertilizer nitrogen to atmospheric nitrous oxide since 1860, Nature Geoscience, 2, 659-662, 2009.

Davidson, E. A., and Kanter, D.: Inventories and scenarios of nitrous oxide emissions, Environmental Research Letters, 9, 105012, 2014.

Dentener, F.: Global maps of atmospheric nitrogen deposition, 1860, 1993, and 2050, Data set. Available on-line (http://daac. ornl. gov/) from Oak Ridge National Laboratory Distributed Active Archive Center, Oak Ridge, TN, USA, 2006.

Duxbury, J., Bouldin, D., Terry, R., and Tate, R. L.: Emissions of nitrous oxide from soils, 1982.

Efron, B., and Tibshirani, R. J.: An introduction to the bootstrap, CRC press, 1994.

Denman K., Brasseur G., Chidthaisong A., Ciais P. M., Cox P., Dickinson R., Hauglustaine D., Heinze C., Holland E., Jacob D., Lohmann U., Ramachandran S., da Silva Dias P., Wofsy S. and Zhang X.: Couplings Between Changes in the Climate System and Biogeochemistry. In: Climate Change 2007: The Physical Science Basis. Contribution of Working Group I to the Fourth Assessment Report of the Intergovernmental Panel on Climate Change [Solomon S., Qin D., Manning M., Chen Z., Marquis M., Averyt K. B., Tignor M., and Miller H. (eds.)]. Cambridge University Press, Cambridge, United Kingdom and New York, NY, USA, 501-566, 2007.

Forster, P., Ramaswamy, V., Artaxo, P., Berntsen, T., Betts, R., Fahey, D. W., Haywood, J., Lean, J., Lowe, D. C., and Myhre, G.: Changes in atmospheric constituents and in radiative forcing. Chapter 2, in: Climate Change 2007. The Physical Science Basis, 2007.

Galloway, J. N., Dentener, F. J., Capone, D. G., Boyer, E. W., Howarth, R. W., Seitzinger, S. P., Asner, G. P., Cleveland, C., Green, P., and Holland, E.: Nitrogen cycles: past, present, and future, Biogeochemistry, 70, 153-226, 2004.

Gerber, S., Hedin, L. O., Oppenheimer, M., Pacala, S. W., and Shevliakova, E.: Nitrogen cycling and feedbacks in a global dynamic land model, Global Biogeochemical Cycles, 24, 2010.

Gerber, J. S., Carlson, K. M., Makowski, D., Mueller, N. D., Garcia de Cortazar-Atauri, I., Havlík, P., Herrero, M., Launay, M., O'Connell, C. S., and Smith, P.: Spatially explicit estimates of N_2O emissions from croplands suggest climate mitigation opportunities from improved fertilizer management, Global Change Biology, 2016.

Hadi, A., Inubushi, K., Furukawa, Y., Purnomo, E., Rasmadi, M., and Tsuruta, H.: Greenhouse gas emissions from tropical peatlands of Kalimantan, Indonesia, Nutrient Cycling in Agroecosystems, 71, 73-80, 2005.

Hall, S. J., and Matson, P. A.: Nitrogen oxide emissions after nitrogen additions in tropical forests, Nature, 400, 152-155, 1999.

Hansen, S.: Daisy, a flexible soil-plant-atmosphere system model, Report. Dept. Agric, 2002.

Heinen, M.: Simplified denitrification models: overview and properties, Geoderma, 133, 444-463, 2006.

Holland, E., Lee-Taylor, J., Nevison, C., and Sulzman, J.: Global N Cycle: Fluxes and N_2O mixing ratios originating from human activity, Data set. Available on-line: http://www. daac. ornl. gov from Oak Ridge National Laboratory Distributed Active Archive Center, Oak Ridge, Tennessee, USA, doi, 10, 2005.

Hu, M., Chen, D., and Dahlgren, R. A.: Modeling nitrous oxide (N_2O) emission from rivers: A global assessment, Global Change Biology, 2016.

Hurtt, G., Chini, L. P., Frolking, S., Betts, R., Feddema, J., Fischer, G., Fisk, J., Hibbard, K., Houghton, R., and Janetos, A.: Harmonization of land-use scenarios for the period 1500–2100: 600 years of global gridded annual land-use transitions, wood harvest, and resulting secondary lands, Climatic Change, 109, 117-161, 2011.

Huttunen, J. T., Alm, J., Liikanen, A., Juutinen, S., Larmola, T., Hammar, T., Silvola, J., and Martikainen, P. J.: Fluxes of methane, carbon dioxide and nitrous oxide in boreal lakes and potential anthropogenic effects on the aquatic greenhouse gas emissions, Chemosphere, 52, 609-621, 2003.

Intergovernmental Panel on Climate Change (IPCC) Revised 1996 IPCC Guidelines for National Greenhouse Gas Inventories vol 1/3 ed J T Houghton, L G Meira Filho, B Lim, K Treanton, I Mamaty, Y Bonduki, D J Griggs and B A Callander (London: IPCC, OECD and IEA), 1997.

Jung, M., Henkel, K., Herold, M., and Churkina, G.: Exploiting synergies of global land cover products for carbon cycle modeling, Remote Sensing of Environment, 101, 534-553, 2006.

Kroeze, C., Mosier, A., and Bouwman, L.: Closing the global N_2O budget: a retrospective analysis 1500–1994, Global Biogeochemical Cycles, 13, 1-8, 1999.

Liu, M., Tian, H., Yang, Q., Yang, J., Song, X., Lohrenz, S. E., and Cai, W. J.: Long-term trends in evapotranspiration and runoff over the drainage basins of the Gulf of Mexico during 1901–2008, Water Resources Research, 49, 1988-2012, 2013.

Lu, C., and Tian, H.: Net greenhouse gas balance in response to nitrogen enrichment: perspectives from a coupled biogeochemical model, Global Change Biology, 19, 571-588, 2013.

Machida, T., Nakazawa, T., Fujii, Y., Aoki, S., and Watanabe, O.: Increase in the atmospheric nitrous oxide concentration during the last 250 years, Geophysical Research Letters, 22, 2921-2924, 1995.

Martikainen, P. J., Nykänen, H., Crill, P., and Silvola, J.: Effect of a lowered water table on nitrous oxide fluxes from northern peatlands, Nature, 366, 51-53, 1993.

Morse, J. L., Durán, J., Beall, F., Enanga, E. M., Creed, I. F., Fernandez, I., and Groffman, P. M.: Soil denitrification fluxes from three northeastern North American forests across a range of nitrogen deposition, Oecologia, 177, 17-27, 2015.

Myhre, G., Shindell, D., Bréon, F., Collins, W., Fuglestvedt, J., Huang, J., Koch, D., Lamarque, J., Lee, D., and Mendoza, B.: Anthropogenic and natural radiative forcing, Climate Change, 423, 2013.

NOAA2006A: Combined Nitrous Oxide data from the NOAA/ESRL Global Monitoring Division, 2016.

Pan, S., Tian, H., Dangal, S. R., Zhang, C., Yang, J., Tao, B., Ouyang, Z., Wang, X., Lu, C., and Ren, W.: Complex Spatiotemporal Responses of Global Terrestrial Primary Production to Climate Change and Increasing Atmospheric CO_2 in the 21 st Century, PloS one, 9, e112810, 2014.

Pan, S., Tian, H., Dangal, S. R., Yang, Q., Yang, J., Lu, C., Tao, B., Ren, W., and Ouyang, Z.: Responses of global terrestrial evapotranspiration to climate change and increasing atmospheric CO_2 in the 21st century, Earth's Future, 3, 15-35, 2015.

Prather, M. J., and Hsu, J.: Coupling of nitrous oxide and methane by global atmospheric chemistry, Science, 330, 952-954, 2010.

Prather, M. J., Holmes, C. D., and Hsu, J.: Reactive greenhouse gas scenarios: Systematic exploration of uncertainties and the role of atmospheric chemistry, Geophysical Research Letters, 39, 2012.

Prather, M. J., Hsu, J., DeLuca, N. M., Jackman, C. H., Oman, L. D., Douglass, A. R., Fleming, E. L., Strahan, S. E., Steenrod, S. D., and Søvde, O. A.: Measuring and modeling the lifetime of nitrous oxide including its variability, Journal of Geophysical Research: Atmospheres, 120, 5693-5705, 2015.

Rahn, T., and Wahlen, M.: A reassessment of the global isotopic budget of atmospheric nitrous oxide, Global Biogeochemical Cycles, 14, 537-543, 2000.

Ravishankara, A., Daniel, J. S., and Portmann, R. W.: Nitrous oxide (N_2O): the dominant ozone-depleting substance emitted in the 21st century, Science, 326, 123-125, 2009.

Reay, D. S., Davidson, E. A., Smith, K. A., Smith, P., Melillo, J. M., Dentener, F., and Crutzen, P. J.: Global agriculture and nitrous oxide emissions, Nature Climate Change, 2, 410-416, 2012.

Ren, W., Tian, H., Xu, X., Liu, M., Lu, C., Chen, G., Melillo, J., Reilly, J., and Liu, J.: Spatial and temporal patterns of CO_2 and CH_4 fluxes in China's croplands in response to multifactor environmental changes, Tellus B, 63, 222-240, 2011.

Rochette, P., Angers, D. A., Bélanger, G., Chantigny, M. H., Prévost, D., and Lévesque, G.: Emissions of N O from Alfalfa and Soybean Crops in Eastern Canada, Soil Science Society of America Journal, 68, 493-506, 2004.

Sawamoto, T., Nakajima, Y., Kasuya, M., Tsuruta, H., and Yagi, K.: Evaluation of emission factors for indirect N_2O emission due to nitrogen leaching in agro-ecosystems, Geophysical Research Letters, 32, 2005.

Schmidt, I., van Spanning, R. J., and Jetten, M. S.: Denitrification and ammonia oxidation by Nitrosomonas europaea wild-type, and NirK-and NorB-deficient mutants, Microbiology, 150, 4107-4114, 2004.

Smith, K. A., and Arah, J.: Losses of nitrogen by denitrification and emissions of nitrogen oxides from soils, Proceedings-Fertiliser Society, 1990.

Spahni, R., Chappellaz, J., Stocker, T. F., Loulergue, L., Hausammann, G., Kawamura, K., Flückiger, J., Schwander, J., Raynaud, D., and Masson-Delmotte, V.: Atmospheric methane and nitrous oxide of the late Pleistocene from Antarctic ice cores, Science, 310, 1317-1321, 2005.

Syakila, A., and Kroeze, C.: The global nitrous oxide budget revisited, Greenhouse Gas Measurement and Management, 1, 17-26, 2011.

Tian, H., Xu, X., Liu, M., Ren, W., Zhang, C., Chen, G., and Lu, C.: Spatial and temporal patterns of CH_4 and N_2O fluxes in terrestrial ecosystems of North America during 1979–2008: application of a global biogeochemistry model, Biogeosciences, 7, 2673-2694, 2010.

Tian, H., Xu, X., Lu, C., Liu, M., Ren, W., Chen, G., Melillo, J., and Liu, J.: Net exchanges of CO_2, CH_4, and N_2O between China's terrestrial ecosystems and the atmosphere and their contributions to global climate warming, Journal of Geophysical Research: Biogeosciences, 116, 2011.

Tian, H., Chen, G., Zhang, C., Liu, M., Sun, G., Chappelka, A., Ren, W., Xu, X., Lu, C., and Pan, S.: Century-scale responses of ecosystem carbon storage and flux to multiple environmental changes in the southern United States, Ecosystems, 15, 674-694, 2012.

Tian, H., Chen, G., Lu, C., Xu, X., Ren, W., Zhang, B., Banger, K., Tao, B., Pan, S., and Liu, M.: Global methane and nitrous oxide emissions from terrestrial ecosystems due to multiple environmental changes, Ecosystem Health and Sustainability, 1, 1-20, 2015.

Tian, H., Lu, C., Ciais, P., Michalak, A. M., Canadell, J. G., Saikawa, E., Huntzinger, D. N., Gurney, K. R., Sitch, S., and Zhang, B.: The terrestrial biosphere as a net source of greenhouse gases to the atmosphere, Nature, 531, 225-228, 2016.

Vitousek, P. M., Menge, D. N., Reed, S. C., and Cleveland, C. C.: Biological nitrogen fixation: rates, patterns and ecological controls in terrestrial ecosystems, Philosophical Transactions of the Royal Society of London B: Biological Sciences, 368, 20130119, 2013.

Volk, C., Elkins, J., Fahey, D., Dutton, G., Gilligan, J., Loewenstein, M., Podolske, J., Chan, K., and Gunson, M.: Evaluation of source gas lifetimes from stratospheric observations, Journal of Geophysical Research: Atmospheres, 102, 25543-25564, 1997.

Wei, Y., Liu, S., Huntzinger, D. N., Michalak, A., Viovy, N., Post, W., Schwalm, C. R., Schaefer, K., Jacobson, A., and Lu, C.: The North American Carbon Program Multi-scale Synthesis and Terrestrial Model

Intercomparison Project–Part 2: Environmental driver data, Geoscientific Model Development, 7, 2875-2893, 2014.

Werner, C., Butterbach-Bahl, K., Haas, E., Hickler, T., and Kiese, R.: A global inventory of N_2O emissions from tropical rainforest soils using a detailed biogeochemical model, Global Biogeochemical Cycles, 21, 2007.

Wrage, N., Velthof, G., Van Beusichem, M., and Oenema, O.: Role of nitrifier denitrification in the production of nitrous oxide, Soil biology and Biochemistry, 33, 1723-1732, 2001.

Yang, Q., Tian, H., Friedrichs, M. A., Hopkinson, C. S., Lu, C., and Najjar, R. G.: Increased nitrogen export from eastern North America to the Atlantic Ocean due to climatic and anthropogenic changes during 1901–2008, Journal of Geophysical Research: Biogeosciences, 120, 1046-1068, 2015.

Zhang, B., Tian, H., Lu, C., Pan, S., Dangal, S.,: Spatial and temporal patterns of livestock manure nitrogen production from 1860 to 2014, in preparation.

Zhang, B., Tian, H., Ren, W., Tao, B., Lu, C., Yang, J., Banger, K., and Pan, S.: Methane emissions from global rice fields: Magnitude, spatiotemporal patterns, and environmental controls, Global Biogeochemical Cycles, 2016.

Zhuang, Q., Lu, Y., and Chen, M.: An inventory of global N_2O emissions from the soils of natural terrestrial ecosystems, Atmospheric Environment, 47, 66-75, 2012.

Clim. Past Discuss., doi:10.5194/cp-2016-103, 2016
Manuscript under review for journal Clim. Past
Published: 24 October 2016

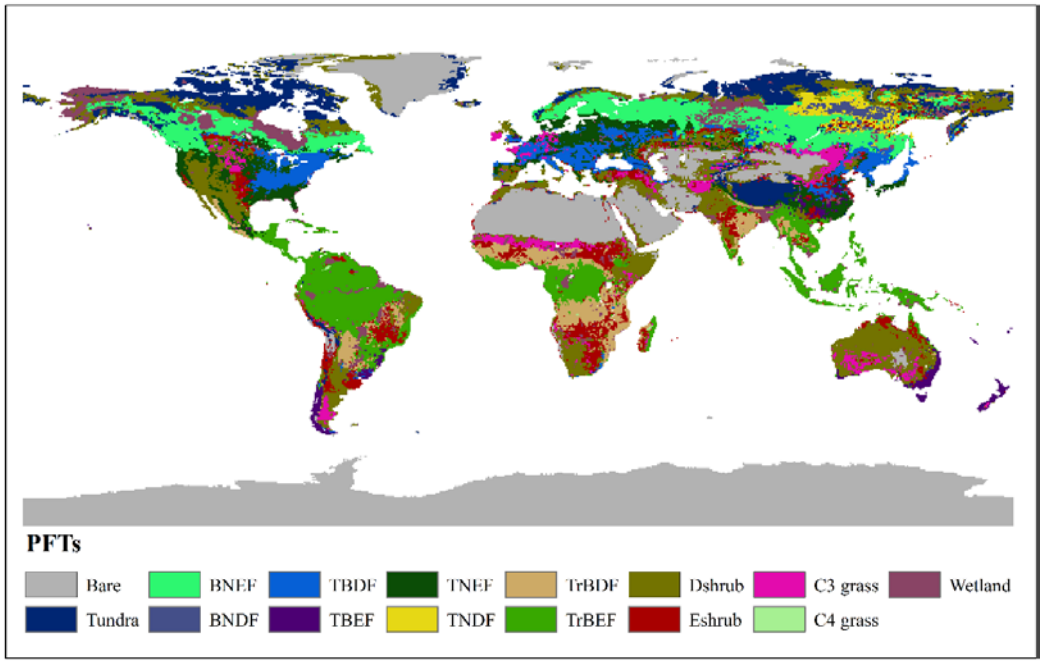

Figure 1. Global potential natural vegetation map used by DLEM in the pre-industrial era. BNEF: Boreal Needleleaf Evergreen Forest, BNDF: Boreal Needleleaf Deciduous Forest, TBDF: Temperate Broadleaf Deciduous Forest, TBEF: Temperate Broadleaf Evergreen Forest, TNEF: Temperate Needleleaf Evergreen Forest, TNDF: Temperate Needleleaf Deciduous Forest, TrBDF: Tropical Broadleaf Deciduous Forest, TrBEF: Tropical Broadleaf Evergreen Forest, Dshrub: Decidous Shrubland, Eshrub: Evergreen Shrubland.

Clim. Past Discuss., doi:10.5194/cp-2016-103, 2016
Manuscript under review for journal Clim. Past
Published: 24 October 2016

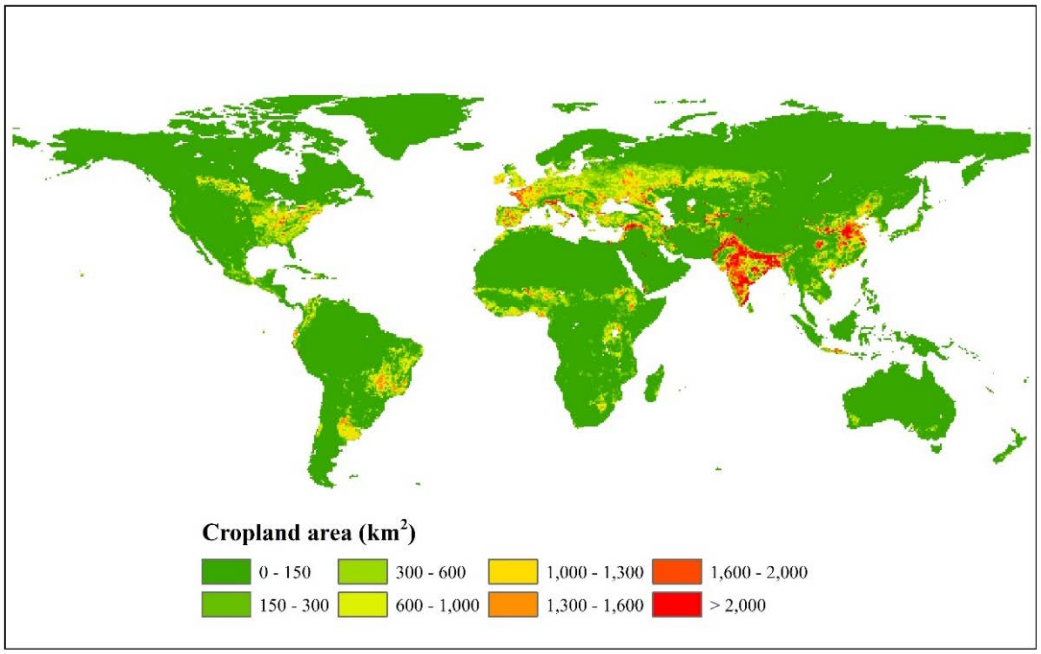

Figure 2. The spatial distribution of cropland area in 1860.

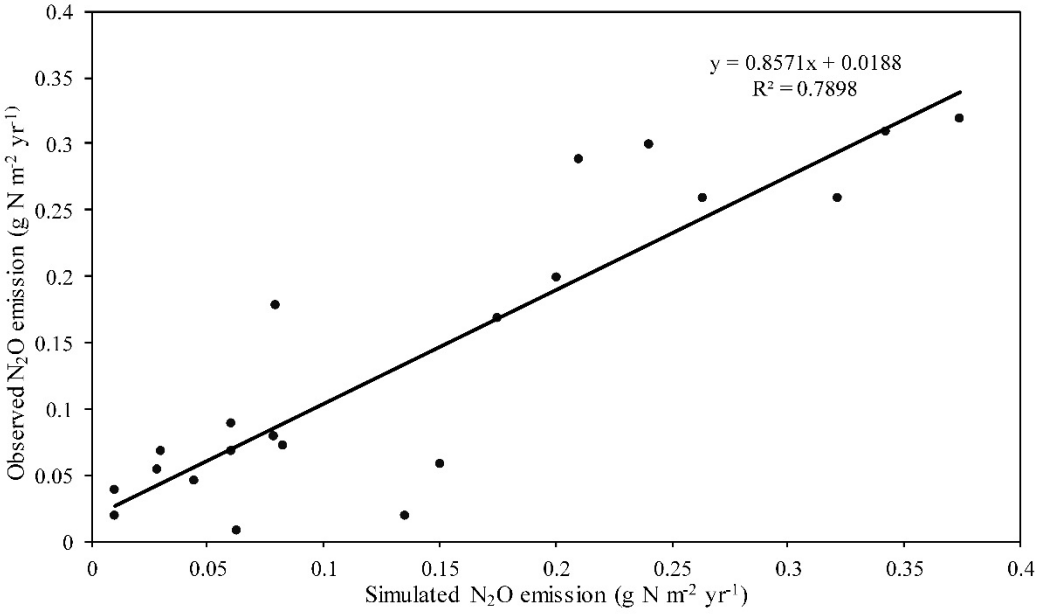

Figure 3. The comparison of the DLEM-simulated N_2O emissions with field observations.

Clim. Past Discuss., doi:10.5194/cp-2016-103, 2016
Manuscript under review for journal Clim. Past
Published: 24 October 2016

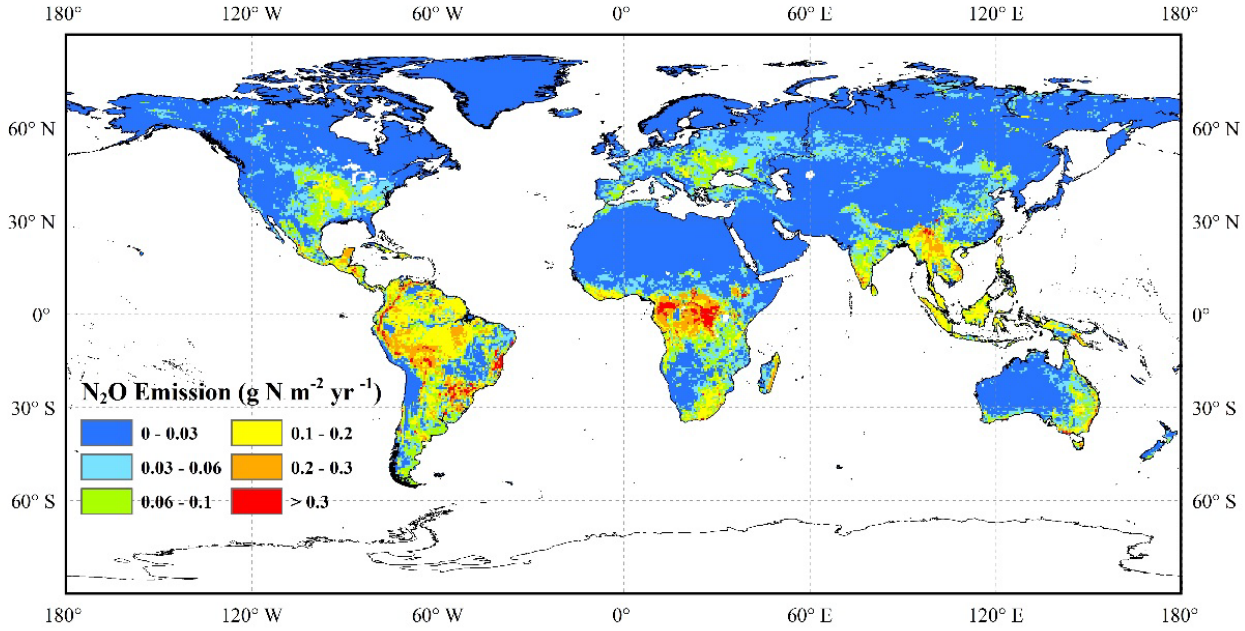

Figure 4. The spatial distribution of N_2O emission in the pre-industrial era.

Clim. Past Discuss., doi:10.5194/cp-2016-103, 2016
Manuscript under review for journal Clim. Past
Published: 24 October 2016

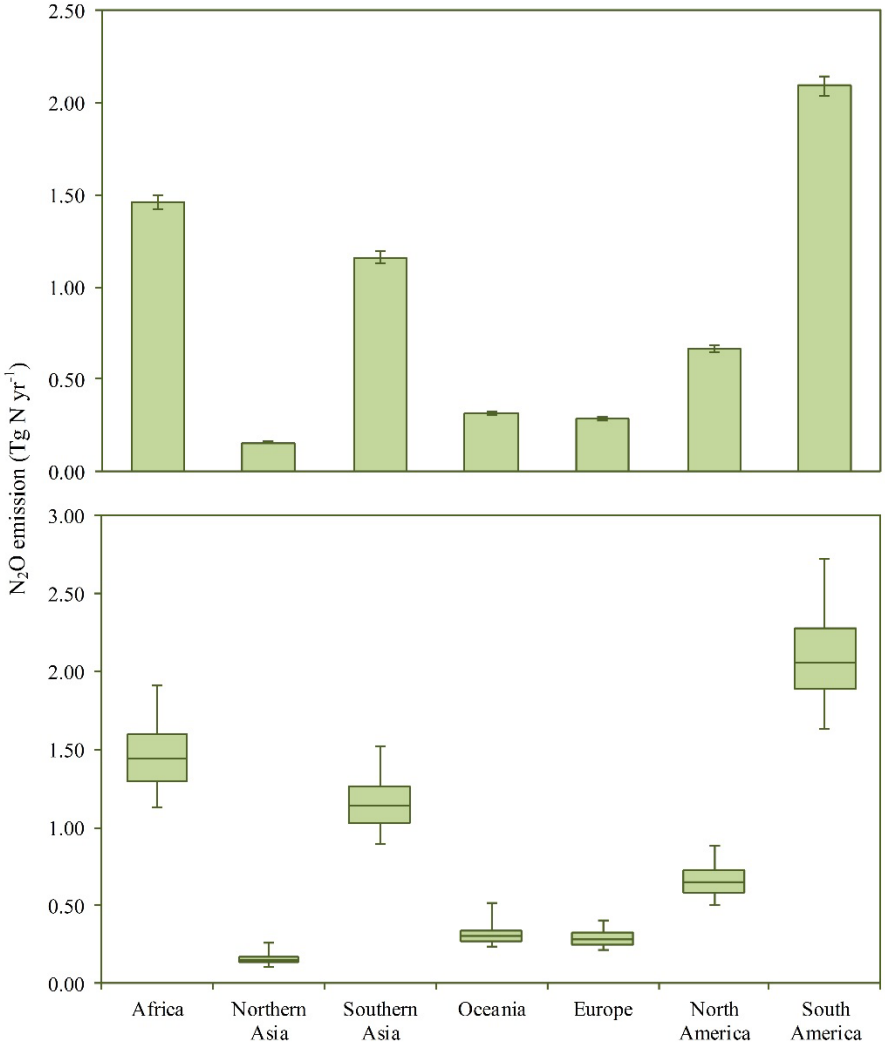

Figure 5. Estimated N_2O emissions at continental-level in 1860: the above graph is the mean emission from different continents with 95% confidence intervals; the below one is the median value and the uncertainty range of emissions.

Clim. Past Discuss., doi:10.5194/cp-2016-103, 2016
Manuscript under review for journal Clim. Past
Published: 24 October 2016

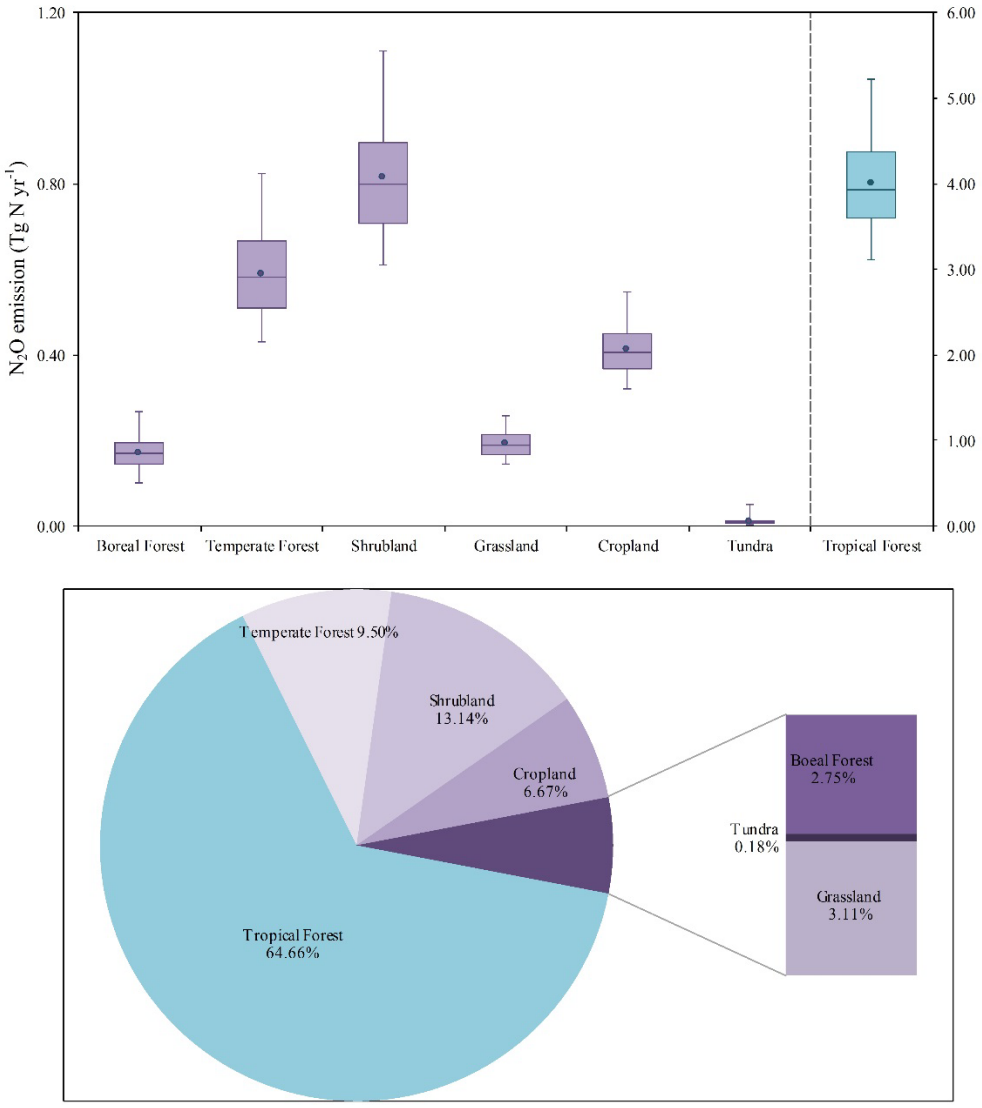

Figure 6. Estimated N_2O emissions at biome-level in 1860: the above graph is the median value (solid line), the mean (solid dot), and the uncertainty range of emissions from different biomes; the below one is the mean percentage of N_2O emissions.

Clim. Past Discuss., doi:10.5194/cp-2016-103, 2016
Manuscript under review for journal Clim. Past
Published: 24 October 2016

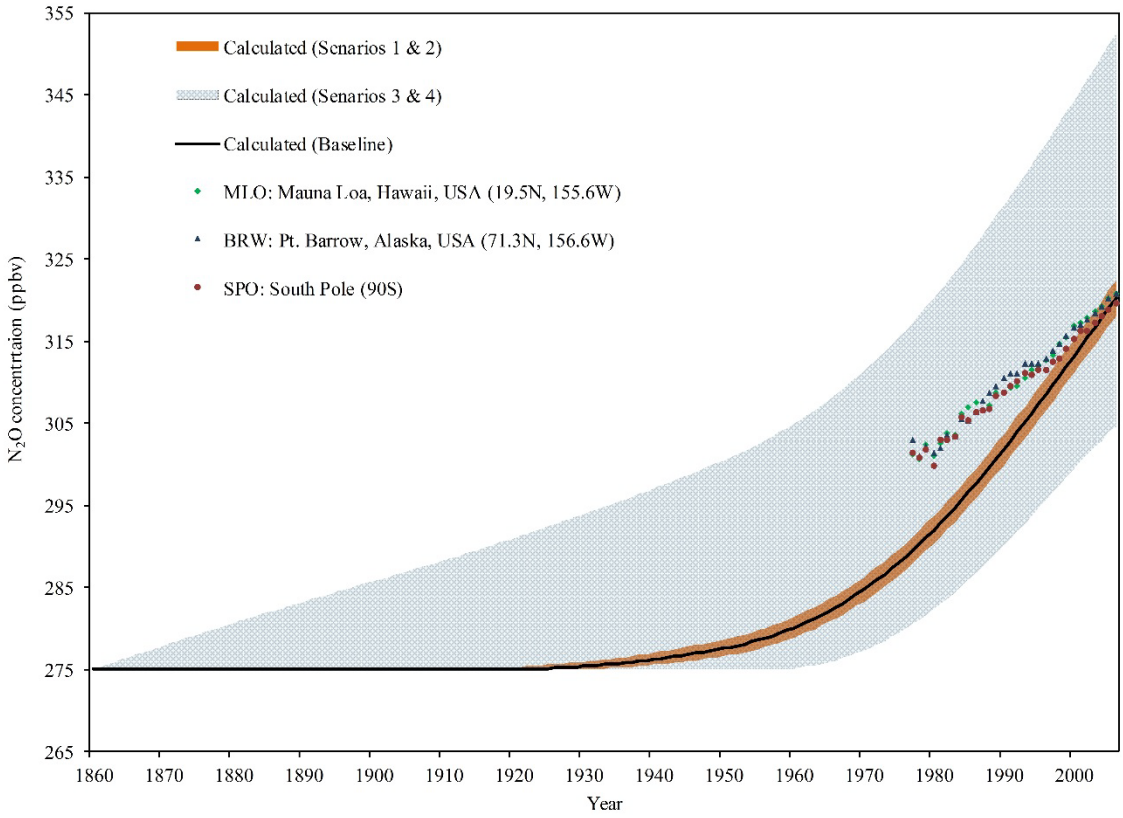

Figure 7. The trends of atmospheric concentration changes in different scenarios as described in Table 1. The method used to retrieve the trends of atmospheric N_2O emission was directly adopted from Syakila and Kroeze (2011) and Kroeze et al. (1999). Similarly, annual emission was linearly interpolated between the years from 1860 to 2006 (net additions of anthropogenic N_2O emission amount in different years were listed in Syakila and Kroeze, 2011). In this study, we focused on confirming the accuracy of pre-industrial estimates, as initial value, from our simulation instead of the accuracy of atmospheric trend itself as discussed in Syakila and Kroeze (2011).

Clim. Past Discuss., doi:10.5194/cp-2016-103, 2016
Manuscript under review for journal Clim. Past
Published: 24 October 2016

Table 1. The estimate ranges of pre-industrial soil emissions, lifetime, and N_2O concentration were used to calculate the concentrations of N_2O in the atmosphere. Baseline was the mean estimate of N_2O emissions from pre-industrial soils through DLEM simulation; Scenarios 1 & 2 were the lower bound and upper bound of the mean estimate, respectively; Scenarios 3 & 4 were the minimum and maximum estimates in this study, respectively; Scenarios 5.1 & 5.2 were the minimum and maximum estimates of N_2O lifetime in the atmosphere, respectively; Scenarios 6.1 & 6.2 were the minimum and maximum estimates of atmospheric N_2O concentration in 1860, respectively.

Scenario	Terrestrial direct N_2O emission (Tg N yr^{-1})	Marine N_2O emission (Tg N yr^{-1})	Other sources (Tg N yr^{-1})	Atmospheric chemistry (Tg N yr^{-1})	Total emission (Tg N yr^{-1})	N_2O life time (years)	Atmospheric N_2O concentration in 1860 (ppb)	Calculated atmospheric 2006 concentration (ppb)
Baseline	6.20	3.5 (before 1950), 4.5 (after 1950)	0.77	0.6	19.27	114	275	320.16
Scenario1	6.03				19.1			318.02
Scenario2	6.36				19.43			322.30
Scenario3	4.76				17.83			304.61
Scenario4	8.13				21.2			352.53
Scenario5.1	6.20				19.27	106	275	309.84
Scenario5.2						141		362.15
Scenario6.1						114	263	314.21
Scenario6.2							280	321.56

Clim. Past Discuss., doi:10.5194/cp-2016-103, 2016
Manuscript under review for journal Clim. Past
Published: 24 October 2016

Table 2. Pre-industrial N_2O emissions from natural vegetation and croplands in different countries.

Country	Vegetation area (Mha)	Natural soils (Gg N yr^{-1})	Cropland (Gg N yr^{-1})	Total (Gg N yr^{-1})
China	756.29	187.60 (Min: 143.13; Max:247.21)	61.74 (Min: 46.65; Max: 83.43)	249.34 (Min: 189.78; Max: 330.64)
India	306.8	120.97 (Min:96.46; Max:153.91)	64.29 (Min: 48.04; Max:86.86)	185.26 (Min: 144.50; Max: 240.77)
United States	913.93	296.45 (Min: 221.19; Max:409.61)	80.95 (Min: 62.38; Max:106.29)	377.40 (Min: 283.57; Max: 515.90)
Pakistan	65.13	5.40 (Min: 4.05; Max:7.30)	6.22 (Min: 4.90; Max:8.16)	11.62 (Min: 8.95; Max: 15.46)
Indonesia	174.07	181.35 (Min: 138.83; Max:237.96)	1.98 (Min: 1.41; Max:2.97)	183.33 (Min: 140.24; Max: 240.93)
France	52.29	6.67 (Min: 4.77; Max:9.49)	8.77 (Min: 6.60; Max:11.84)	15.44 (Min: 11.37; Max: 21.33)
Brazil	835.13	1016.53 (Min: 791.25; Max:1321.97)	10.50 (Min: 8.00; Max:14.20)	1027.03 (Min: 799.25; Max: 1336.17)
Canada	914.61	93.96 (Min: 60.85; Max:137.00)	2.47 (Min: 1.75; Max:3.49)	96.43 (Min: 62.60; Max: 140.49)
Germany	35.99	8.56 (Min: 6.22; Max:12.22)	4.27 (Min: 3.18; Max:5.88)	12.83 (Min: 9.40; Max: 18.10)
Turkey	74.26	17.02 (Min: 12.37; Max:24.07)	10.89 (Min: 8.42; Max:14.32)	27.91 (Min: 20.79; Max: 38.39)
Mexico	190.98	118.13 (Min: 90.56; Max:155.64)	2.93 (Min: 2.43; Max:3.58)	121.06 (Min: 92.99; Max: 159.22)
Vietnam	31.71	41.38 (Min: 33.00; Max:53.27)	2.15 (Min: 1.60; Max:2.84)	43.53 (Min: 34.60; Max: 56.11)
Spain	48.24	14.30 (Min: 10.70; Max:19.46)	5.64 (Min: 4.23; Max:7.68)	19.94 (Min: 14.93; Max: 27.14)
Russian Federation	1575.27	233.98 (Min: 164.71; Max:333.24)	19.28 (Min: 14.39; Max:26.20)	253.26 (Min: 179.10; Max: 359.44)
Bangladesh	12.41	1.61 (Min: 1.31; Max:2.02)	5.38 (Min: 3.87; Max:7.59)	6.99 (Min: 5.18; Max: 9.61)
Thailand	49.26	55.87 (Min: 44.57; Max:71.77)	2.62 (Min: 1.96; Max:3.56)	58.49 (Min: 46.53; Max: 75.33)